Food and Bioprocess Technology, 11, 603-609.

https://doi.org/10.1007/s11947-017-2033-x

Pulsed light inactivation of mushroom polyphenol oxidase: a fluorometric and spectrophotometric study

José Antonio Pellicer[a], Patricia Navarro[a] and Vicente M. Gómez-López[b]

[a] Departamento de Ciencia y Tecnología de Alimentos, Universidad Católica de Murcia (UCAM), Campus de los Jerónimos 135, Guadalupe 30107, Murcia, Spain.

[b] Cátedra Alimentos para la Salud, Universidad Católica de Murcia (UCAM), Campus de los Jerónimos 135, Guadalupe 30107, Murcia, Spain.

Corresponding author:

Vicente M. Gómez-López, phone: + 34 968 278 638, vmgomez@ucam.edu

Other authors:

José Antonio Pellicer, japellicer@ucam.edu

Patricia Navarro, PNavarro@ucam.edu

Abstract

Polyphenol oxidase (PPO) is one of the most important food enzymes, it is responsible for the browning of many foods. Pulsed light (PL) is a non-thermal method of food preservation that is able to inactivate PPO. The aim of this work was to gain insight into the mechanism of PPO inactivation by PL. To this, the kinetics of PPO inactivation by PL was measured, together with associated changes in tryptophan fluorescence, KI fluorescence quenching and turbidity; and results were analysed by parameter A and phase diagram methods. Enzyme inactivation followed the Weibull model. Tryptophan fluorescence decreased during PL treatment, as well as the parameter A, while Stern-Volmer constants increased and turbidity was constant. The phase diagram showed only two populated states. There was a high correlation between the loss of activity and parameter A. Results indicate that under the experimental conditions, the inactivation of PPO by PL is an all-or-none process where the enzyme progressively unfolds with no evidence of aggregation.

Keywords: pulsed light; polyphenol oxidase; enzyme inactivation; enzyme structure; fluorescence spectroscopy.

1. Introduction

Pulsed light (PL) technology is a non-thermal method of food processing based on the application of one or more pulses of high-intensity wide-spectrum light encompassing from UV to infrared (Gómez-López et al. 2007). The application of PL has been mainly focused on microbial inactivation, but its scope of application has increased in the last years to uses such as enzyme inactivation (Manzocco et al. 2013a; Pellicer and Gómez-López 2017) and even to fields with no relation to food technology such as the decrease of environmental pollution (Navarro et al. 2017). PL treatments are characterized in fluence units, which is defined by IUPAC as: "the total radiant energy traversing a small transparent imaginary spherical target containing the point under consideration, divided by the cross section of this target" (Braslavsky 2007).

Polyphenol oxidase (PPO, E.C. 1.14.18.1) is one of the most important enzymes in food technology. It catalyzes the oxidation of phenols to quinones, which undergo a series of reactions leading to browning. PPO is a copper containing enzyme characterized by a quaternary structure composed of four sub-units, two "heavy" chains called H subunits and two "light" chains called L subunits (Mayer and Harel 1979).

The use of PL for PPO inactivation was mentioned by first time in 1989 in a US Patent by Dunn et al. (1989), where the application of PL to potato slices prevented browning and decreased extractable PPO activity. Later on, Manzocco et al. (2013a) reported on the inactivation of PPO by PL *in vitro*, finding that it is a concentration dependent process where the inactivation is faster at low enzyme concentrations, which was attributed to a crowding effect and in minor extent to the shadowing effect. Little is known about the structural changes associated to enzyme inactivation by PL and inactivation studies have been accompanied by a limited or absent use of analytical techniques for protein structure elucidation. Manzocco et al. (2013a) used HPLC-gel permeation to explain PPO

inactivation by PL; they attributed the loss of enzymatic activity to both unfolding/aggregation phenomena and protein backbone cleavage. The PL inactivation of lipoxygenase (LOX) was accounted by protein fragmentation while ruling out the possibilities of cross-linking, agglomeration and polymerization (Janve et al. 2014), according to results found by SDS-electrophoresis and reverse phase HPLC. The loss of activity of peroxidase after PL treatment is an all-or-none process related to loss of helical structure, unfolding and ejection of the hemin prostetic group (Pellicer and Gómez-López 2017). The inactivation of alkaline phosphatase by PL has also been reported but not the promoted structural changes (Innocente et al. 2014).

The inactivation of PPO by PL has been tested not only *in vitro*, but also in fresh-cut fruits and mushrooms, where a decrease of PPO activity has been determined (Oms-Oliu et al. 2010) or the arrest of enzymatic browning can be associated with PPO inactivation (Gómez et al. 2012).

Fluoroscopy and spectrophotometry are two methods used to study structural changes of enzymes. Fluorescence spectroscopy is a very useful technique to study structural changes caused by food processing methods on enzymes. Tryptophan (Trp) fluorescence is the preferred internal probe in fluorescence spectroscopy of proteins because it is the most abundant of three fluorescencent aminoacids, it has a high absorptivity and a high quantum yield (Ghisaidoobe and Chung 2014). Furthermore, and very importantly, tryptophan spectroscopic properties are highly sensitive to the local environment, which makes it a very useful probe for monitoring protein unfolding. The contribution to the Trp intrinsic fluorescence intensity of native PPO is provided by 22 Trp residues; of these, 10 are completely or partially exposed to the solvent and none are located on the subunit interfaces (Ionită et al. 2014a). On the other hand, visible absorption spectroscopy has been used to monitor protein aggregation (Manzocco et al. 2013b; Siddique et al. 2017).

Manzocco et al. (2013a) has provided a first sight on the structural changes that PPO undergoes when treated by PL. Given the importance of this enzyme in the food processing industry, a deeper insight into the structural changes promoted by PL on this enzyme is deserved. In the present work, it was studied the emissive properties of commercial PPO, focusing on structural changes promoted by PL treatment. To this, intrinsic fluorescence, the parameter A, the phase diagram method, fluorescence quenching experiments using iodide and absorption spectra were the analytical tools used. The results were correlated to the inactivation kinetics.

2. Materials and Methods

2.1. Reagents

Mushroom PPO (T3824, Sigma-Aldrich), a commercial product isolated from the mushroom *Agaricus bisporus*, was used through the study. Other reagents were also purchased from Sigma-Aldrich. A stock PPO solution (31.5 µg/ml) was prepared in 0.1 M phosphate buffer pH 6.5. Since results can be affected by enzyme concentration, the stock solution was prepared once for the whole study. It was separated in small portions in Eppendorf flasks and stored at -20 ºC until usage. The same sample was used for different determinations whenever was possible.

2.2. Apparatus

PPO samples were treated with PL in a XeMaticA-Basic-1L system (Steribeam, Kehl, Germany) (fig. 1). The treatment chamber of this system is 20 cm wide, 14 cm high and 10 cm deep and has one 19-cm long xenon lamp placed at the top of the chamber. A stirrer (Topolino, IKA, Staufen, Germany) was incorporated to the chamber as platform for holding sample plates and for inter-pulse sample homogenization. The system generates

pulses of 200 µs of a polychromatic light with spectral composition ranging from infrared to ultraviolet light. It was operated at a discharge voltage of 2.5 kV, which generates 500 J/pulse of light with 21% of UV component. The characteristic emission spectrum of the lamp under these working conditions has been reported before (Cudemos et al. 2013). Samples received an incident fluence of 2.14 J/cm^2 pulse, which was determined by analysis of in-built photodiode readings using a PC-Lab 2000 LT PC oscilloscope (Velleman Instruments, Gavere, Belgium), and manufacturer performance charts. Different fluencies were obtained by increasing the number of pulses up to 60.

2.3. Experimental procedure

A Petri dish without cover with 20 mL of PPO solution was placed on the stirrer below the centre of the lamp. This volume (2.7 mm height) was selected as the minimum required to fully covering the bottom of the dish. The distance between the lamp and the sample surface was 6.7 cm. Temperature through treatments was monitored by an infrared thermometer (ScanTemp 410, TFA Dostmann, Wertheim, Germany) according to a standardized procedure (Pellicer and Gómez-López 2017).

2.4. Enzymatic activity

PPO activity was measured at 400 nm in a standard reaction mixture containing 100 mM sodium phosphate buffer (pH 6.5), enzyme sample and 2.5 mM of 4-tert-butyl catechol. One unit of enzyme activity (U) will be defined as the amount of enzyme that produces 1 µmol of tert-butyl-o-quinone per minute (Núñez-Delicado et al. 2007). The residual PPO activity was computed using equation 1:

$$\%\, residual\ PPO\ activty = \frac{U_F}{U_o}\ x\ 100 \qquad (1)$$

where, U_o is the enzymatic activity without treatment and U_F is the enzymatic activity after a treatment of fluence F. Spectrophotometric measurements were carried out by using a UV-Vis spectrophotometer (UV-1700, Shimadzu, Japan).

The enzymatic activity was measured every five pulses during treatment for inactivation kinetics, and then for 30, 60 and 90 min post-treatment on samples stored in darkness in order to assess potential reactivation. Fluence (F_o, J/cm^2) is related to number of pulses and treatment time (t, sec) by the following formula:

$$F_o = F_{o,\pi}\, f\, t \qquad (2)$$

where $F_{o,\pi}$ is the fluence per pulse and f (Hz) is the pulse repetition rate. The number of pulses is $f\,t$.

2.5. Steady-state tryptophan fluorescence spectroscopy

Intrinsic Trp fluorescence was used to characterize potential changes in the tertiary structure of the enzymes. Trp fluorescence spectra was measured with a spectrofluorimeter model RF-Shimadzu 5301 PC (Shimadzu, Japan), using a quartz cuvette of 1 cm optical path-length at room temperature (25 ˚C). All samples were measured after 0, 10, 20, 30, 40, 50 and 60 light pulses. Determinations were carried out with a sampling interval of 1 nm and slits of 5 nm. The excitation wavelength was set to 293 nm and the fluorescence emission spectra were scanned from 300 to 450 nm.

Phase diagrams

Phase diagrams were constructed using intrinsic fluorescence spectra data to probe if the structural transformation of the PPO from native to inactive form follows an all-or-none or a multi-step process. The phase diagram method is based on the equation:

$$I(\lambda_1) = a + b\, I(\lambda_2) \qquad (3)$$

where $I(\lambda_1)$ and $I(\lambda_2)$ are the spectral intensities at wavelengths λ_1 and λ_2 under different fluences and *a* and *b* are the intercept and the slope respectively of the $I(\lambda_1)$ versus $I(\lambda_2)$ plot (Kuznetsova et al. 2004).

2.6. **Parameter** A

Fluorescence changes were also characterized in terms of parameter A (Turoverov et al. 1976) according to equation 4:

$$parameter\ A = (\frac{I_{320}}{I_{365}})_{293} \qquad (4)$$

where I_{320} and I_{365} are fluorescence intensities at emission wavelengths of 320 and 365 nm respectively for an excitation wavelength set to 293 nm. This parameter is used in structural protein studies to characterize the position and form of fluorescence spectra.

2.7. **KI fluorescence quenching**

Fluorescence quenching experiments were performed with freshly prepared 5 M KI in 10 mM Tris-HCl buffer at pH 7.0. Quenching titrations were performed by adding different volumes of KI solution to untreated and PL treated PPO samples and gently stirring. Fluorescence measurements were performed with an excitation wavelength set at 292 nm and emission wavelengths in the range 300-450 nm.

Data were analysed by fitting to the Stern-Volmer equation:

$$\frac{F_0}{F} = 1 + K_{SV}\,[KI] \qquad (45)$$

where F_0 and F are the fluorescence intensities in the absence and presence of quencher, *[KI]* (M) is the concentration of KI and K_{SV} (M^{-1}) is the Stern-Volmer quenching constant (Ionită et al. 2014a).

2.8. **Spectrophotometric measurements**

UV-vis spectra of untreated and PL treated samples were recorded in the UV-1700 spectrophotometer using a quartz cuvette with a 1 cm path length. Turbidity was measured as absorbance at 420 nm (Ju and Kilara 1998).

2.9. Data analysis

Data of inactivation curve were fitted to the Weibull model. The Weibull structure reads as follows:

$$\log(U_F) = \log U_0 - (F/\delta)^p \qquad (5\text{~~5~~}6)$$

where δ (J/cm^2) is the incident fluence for obtaining the first decimal reduction and p (dimensionless) is a parameter describing convexity (p > 1) or concavity (p < 1) of the curve. Data was processed using GInaFIT add-in tool for Excel (Geeraerd et al. 2005). Other data fitting was carried out in Microsoft Excel 2016. Turbidity values and Stern-Volmer constants were analysed by one-way ANOVA and Duncan test with P<0.05 using IBM Statgraphics 24. Each experiment was repeated three times.

3. Results and Discussion

3.1. Kinetics of PPO inactivation by PL

The inactivation of PPO by PL (fig. 2) was first fitted to a first-order kinetics, which yielded a rate equal to 0.0175 cm^2/J with a R^2=0.9925 and a Root Mean Sum of Squared Error (RMSE) of 0.0286. Similarly, the PL inactivation of LOX under three different conditions was fitted by Janve et al. (2014) to the first-order kinetic model with R^2>0.98. However, it was obvious in the current case that a small shoulder was not fitted by the model, perhaps due to the existence of isoenzymes with different stability towards PL.

Therefore, the suitability of using the Weibull model was tested to better data fit. The Weibull model fitted inactivation data satisfactorily, with a R^2=0.9999 and a RMSE of 0.0055. Weibull parameters were δ= 133.0 ± 0.9 J/cm^2 and p=1.24±0.05. The Weibull distribution was first used to describe microbial inactivation, but has also been used to model the kinetic of enzyme inactivation by non-thermal methods such as pulsed electric fields (Elez-Martínez et al. 2006), cold plasma (Cullen et al. 2013) and UV-C light (Sampedro and Fan 2014) but not for PL. Awareness of inactivation curves different to the classic first-order inactivation kinetics is important to avoid miscalculations of treatment conditions when upscaling to industrial applications. Temperature increase was less than 3 ºC, which rules out any thermal effect on the enzyme inactivation observed in this study.

The definition of treatment conditions is extremely important in experiments of PPO inactivation by PL since the shape of the inactivation curve and the inactivation rate strongly depends on enzyme concentration according to Manzocco et al. (2013a), likely due to the crowding effect. Nearly 90 % inactivation was achieved after applying 128 J/cm^2. This fluence is higher than that reported by Manzocco et al. (2013a). Besides concentration effects, two other reasons can explain this large difference. One of the reasons is the difference in the target configuration. While those authors used aliquots of 100 µL of enzyme solutions inside 2 x 3 cm plastic pouches with no stirring, the current study used 20 ml of enzyme solution in uncovered Petri dishes with stirring, therefore, having different lengths of the light path. Another reason is caused by the lack of accuracy in fluence determinations in bench-top PL systems inherent to the absence of a standardized protocol as it has been recently discussed (Gómez-López and Bolton 2016).

3.2. Intrinsic tryptophan fluorescence spectroscopy

Intrinsic Trp fluorescence is frequently used as an internal fluorescence probe to study the tertiary structure of proteins, with the advantage of avoiding potential conformational changes induced by extrinsic probes (Ionită et al. 2014a). Trp fluorescence intensity depends on the environment where it is. When the aminoacid is buried inside protein structure is in a hydrophobic environment, where its quantum yield is high and consequently the intensity of its fluorescence is high. When proteins unfold, Trp gets exposed to a hydrophilic environment, where its quantum yield is low and therefore its fluorescence decreases. Fig. 3 shows the change of fluorescence spectrum as function of fluence. The spectrum flattens with increasing fluence, which is an evidence that PPO is unfolded by PL treatment. The maximum emission wavelength (λ_{max}) for the native PPO is 328 nm and decreased by 58 % at the end of the treatment. No peak shifts were observed during processing in spite of the decrease in fluorescence intensity due to the exposure of buried Trp residues to a hydrophilic environment is generally accompanied by a red shift (Ghisaidoobe and Chung 2014). However, this is not always the case, likely because water exposure *per se* is not sufficient for a red shift (Vivian and Callis 2001). Interestingly, the fluorescence spectrum (but using an excitation wavelength set at 280 nm, which excites not only Trp but also phenylalanine and tyrosine) of the inactivation of PPO by monochromatic UV light (254 nm) (Haddouche et al. 2015) also shows no λ_{max} shifts.

The spectral parameter A is a quantitative characteristic of the fluorescence spectrum of protein Trp residues, it is together with λ_{max} an useful tool to characterize the fluorescence spectrum (Turoverov et al. 1976). Fig. 4 shows that the parameter A decreases in a way directly proportional to the progress of the treatment, which indicates that the changes in the tertiary structure of the PPO during PL treatment are proportional to the amount of photons impinging the protein.

Fig. 5 shows how the observed changes in parameter A are highly correlated to residual PPO activity. The same plot replacing parameter A by peak fluorescence intensity has also a high correlation coefficient (> 0.99). Since PPO inactivation by PL is sensitive to enzyme concentration (Manzocco et al. 2013a), this kind of correlations can only be established between samples at the same PPO concentration; for this reason, precaution was taken to prepare a single PPO solution for the whole study. The high correlation of PPO inactivation with changes in Trp intrinsic fluorescence (R^2>0.99) leads to conclude that protein unfolding is the responsible of PPO inactivation by PL under the assay conditions. Yet, this conclusion does not rule out changes at other structural levels.

Even though the results show that the loss of PPO activity upon PL treatment are clearly related to enzyme unfolding, the possibility of protein aggregation should be considered since it has been reported for this specific case as described by Manzocco et al. (2013a). No evidence of aggregation for this protein can be derived from fig. ~~2~~3. If PPO aggregation had occurred, an increase of fluorescence would have been expected due to the burial of Trp residues at the aggregation zones of the surface of the enzyme.

3.3. Phase diagram

The phase diagram method is used to describe the unfolding pathway of a protein. This method predicts that the dependence of $I(\lambda_1) = f(I(\lambda_2))$ will be linear if changes lead to all-or-none transition between two different conformations. If several lines are found, the change is a multistate process, each line reflecting a two-state process which intersections are populated by intermediate forms of the enzyme in the way to the progress of its inactivation (Kuznetsova et al. 2002; Jiang et al. 2008). Fig. 6 shows the phase diagram for the inactivation of PPO by PL under the assay conditions. Since both, I_{320} and I_{365}, are dependent variables, values do not match among replicates and results could not be averaged. It can be seen that the diagram is linear and the ratio I_{365}/I_{320} continuously

decreased with increasing fluence. This finding shows that the inactivation of PPO by PL is an all-or-none process. This conclusion is further supported by the analysis of the evolution of parameter A versus fluence (fig. 4), in which a linear plot shows no indicium of the accumulation of intermediates (Kumar and Gaikwad 2010).

3.4. Fluorescence quenching

To further investigate the inactivation of PPO by PL, fluorescence quenching by KI was investigated. KI is an ionic quencher that can extinguish only fluorescence emitted by fluorophores located at, or near to, the surface of molecules (Ionită et al. 2014a). The variation of fluorescence intensity with KI followed the Stern-Vomer equation without change in the spectral shape. Table 1 shows the Stern-Volmer constants for untreated and PL treated enzyme at intermediate and final fluences. The Stern-Volmer constant was equal for the first two conditions ($P>0.05$) and doubled at the final fluence. The increase of quenching constant indicates protein unfolding, which decreases the distance between Trp residues and the quencher (Ionită et al. 2014b) and shows no evidence of aggregation, which would have decreased quenching by hiding surficial Trp residues.

3.5. Turbidity

Turbidity measurements have been used to assess the formation of protein aggregates produced by covalent and no-covalent interactions (Sidiqque et al. 2017). Measuring absorbance at 420 nm has been shown to be sensitive to protein aggregation (Ju and Kilara 1998) used it to measure aggregation of a whey protein solution upon addition of $CaCl_2$, with initial absorbances of less than 0.05, which can increase up to 1.6 when aggregation was promoted. Table 1 shows turbidity measurements after treating PPO to increasing PL fluences. It can be observed that there was no change in the turbidity index ($P>0.05$), which implies no evidence of protein aggregation due to PL. This is not the case for all proteins treated by PL. An increase of 9 % in absorbance at 420 nm has been reported for

whey protein isolate (Siddique et al. 2017), while the turbidity of egg white measured at 680 nm increased six fold (Manzocco et al. 2013b).

Even though the different analytical tools used in the current study show no evidence of protein aggregation as reported earlier (Manzocco et al. 2013a), both works do not contradict each other, because differences in PPO concentrations may account for this divergent results. For example, the aggregation of α-amylases upon heating is less pronounced at lower protein concentrations (Duy and Fitter 2006). If proteins are highly diluted, their possibility to interact with each other to form aggregates would be low. The possibility of intermolecular cross-linking increases at higher concentrations until the system reaches the crowding concentration, which can make it photostable (Manzocco 2015). New experiments under different enzyme concentrations applying a wide array of structural analytical tools are foreseen.

4. Conclusions

The inactivation of PPO by PL was studied by means of fluorometric and spectrophotometric techniques. PPO inactivation by PL shows an inactivation phase preceded by a shoulder, likely because of the presence of isoenzymes with different photostability, and which kinetic was fitted by the Weibull model. The loss of PPO activity was highly correlated to protein unfolding as measured by Trp intrinsic fluorescence. The linearity of both, the phase diagram and the plot of parameter A vs fluence indicate that the PL inactivation of PPO is an all-or-none process. No evidence of aggregation was observed when measuring intrinsic fluorescence, KI fluorescence quenching and turbidity. Results indicate that the PL inactivation of PPO is caused by an all-or-none process of protein unfolding with no enzyme aggregation under the

experimental conditions. Discrepancies with previous works might be related to differences in used enzyme concentrations.

Acknowledgments

This work was supported by Universidad Católica de Murcia, grant PMAFI/29/14.

References

Braslavsky, S. E. (2007). Glossary of terms used in photochemistry. *Pure & Applied Chemistry, 79*, 293–465.

Cudemos, E., Izquier, A., Medina-Martínez, M. S., & Gómez-López, V. M. (2013). Effects of shading and growth phase on the microbial inactivation by pulsed light. *Czech Journal of Food Sciences, 31*, 189-193.

Cullen, P.J., Pankaj, S.K., & Misra, N.N. (2013). Kinetics of tomato peroxidase inactivation by atmospheric cold plasma based on dielectric barrier discharge. *Innovative Food Science and Emerging Technologies, 19*, 153-157.

Dunn, J., Clark, R.W., Asmus, J.F., Pearlman, J.S., Boyer, K., Painchaud, F., & Hofmann, G.A. (1989). Methods for preservation of foodstuffs. *US patent 4,871,559*.

Duy, C., & Fitter, J. (2006). How aggregation and conformational scrambling of unfolded states govern fluorescence emission spectra. *Biophysical Journal, 90*, 3704-3711.

Elez-Martínez, P., Aguiló-Aguayo, I., & Martín-Belloso, O. (2006). Inactivation of orange juice peroxidase by high-intensity pulsed electric fields as influenced by process parameters. *Journal of the Science of Food and Agriculture, 86*, 71-81.

Geeraerd, A.H., Valdramidis, V.P., & Van Impe, J.F. (2005). GInaFIT, a freeware tool to assess non-log-linear microbial survivor curves. *International Journal of Food Microbiology, 102*, 95-105.

Ghisaidoobe, A.B.T, & Chung, S.J. (2014). Intrinsic tryptophan fluorescence in the detection and analysis of proteins: a focus on Förster resonance energy transfer techniques. *International Journal of Molecular Sciences, 15*, 22518-22538.

Gómez, P.L., Salvatori, D.M., García-Loredo, A., & Alzamora, S.M. (2012). Pulsed light treatment of cut apple: dose effect on color, structure, and microbiological stability. *Food and Bioprocess Technology, 5*, 2311-2322.

Gómez-López, V.M., & Bolton, J.R. (2016). An approach to standardize methods for fluence determination in bench-scale pulsed light experiments. *Food and Bioprocess Technology*, *9*, 1040-1048.Gómez-López, V.M., Ragaert, P., Debevere, J., & Devlieghere, F. (2007). Pulsed light for food decontamination: a review. *Trends in Food Science and Technology, 18*, 464-473.

Innocente, N., Segat, A., Manzocco, L., Marino, M., Maifreni, M., Bortolomeoli, I., Ignat, A., & Nicoli, M.C. (2014). Effect of pulsed light on total microbial count and alkaline phosphatase activity of raw milk. *International Dairy Journal*, *39*, 108-112.

Haddouche, L., Phalak, A., & Tikekar, R.V. (2015). Inactivation of polyphenol oxidase using 254 nm ultraviolet light in a model system. *LWT-Food Science and Technology*, *62*, 97-103.

Ionită, E., Stănciuc, N., Aprodu, I., Râpeanu, G., & Bahrim, G. (2014a). pH-induced structural changes of tyrosinase from *Agaricus bisporus* using fluorescence and *in silico* methods. *Journal of the Science of Food and Agriculture, 94*, 2338-2344.

Ionită, E., Aprodu, I., Stănciuc, N., Râpeanu, G., & Bahrim, G. (2014b). Advances in structure-function relationships of tyrosinase from *Agaricus bisporus* – Investigation on heat-induced conformational changes. *Food Chemistry, 156*, 129-136.

Janve, B.A., Yang, W., Marshall, M.R., Reyes-De-Corcuera, J.I., & Rababah, T.M. (2014). Nonthermal inactivation of soy (*Glycine max* sp.) lipoxygenase by pulsed ultraviolet light. *Journal of Food Science, 79*, C8-C18.

Jiang, Y., Su, J.T., Zhang, J., Wei, X., Yan, Y.B., & Zhou, H.M. (2008). Reshaping the folding energy landscape of human carbonic anhydrase II by a single point genetic mutation Pro237His. *The International Journal of Biochemistry & Cell Biology, 40*, 776-788.

Ju, Z.Y., & Kilara, A. (1998). Aggregation induced by calcium chloride and subsequent thermal gelation of whey protein isolate. *Journal of Dairy Science, 81*, 925-931.

Kumar, A., & Gaikwad, S.M. (2010). Multistate unfolding of α-mannosidase from *Canavalia ensiformis* (Jack Bean): evidence for the thermostable molten globule. *Biochemical and Biophysical Research Communications, 403*, 391-397.

Kuznetsova, I.M., Stepanenko, O.V., Turoverov, K.K., Zhu, L., Zhou, J.M., Fink, A.L., & Uversky, V.N. (2002). Unraveling multistate unfolding of rabbit muscle creatine kinase. *Biochimica et Biophsica Acta, 1596*, 138-155.

Kuznetsova, I., Turoverov, K.K., & Uversky, V.N. (2004). Use of the phase diagram method to analyse the protein unfolding-refolding reactions: fishing out the "invisible" intermediates. *Journal of Proteome Research, 3*, 485-494.

Manzocco, L. (2015). Photo-induced modification of food protein structure and functionality. *Food Engineering Reviews, 7*, 346-356.

Manzocco, L., Panozzo, A., & Nicoli, M.C. (2013a). Inactivation of polyphenol oxidase by pulsed light. *Journal of Food Science, 78*, E1183-E1187.

Manzocco, L., Panozzo, A., & Nicoli, M.C. (2013b). Effect of pulsed light on selected properties of egg white. *Innovative Food Science and Emerging Technologies, 18*, 183-189.

Mayer, A.M., & Harel, E. (1979). Polyphenol oxidases in plants. *Phytochemistry, 18*, 193-215.

Núñez-Delicado, E., Serrano-Megías, M., Pérez-López, A. J., & López-Nicolás, J. M. (2007). Characterization of polyphenol oxidase from Napoleon grape. *Food Chemistry, 100*, 108-114.

Navarro, P., Gabaldón, J.A., & Gómez-López, V.M. (2017). Degradation of an azo dye by a fast and innovative pulsed light/H_2O_2 advanced oxidation process. *Dyes and Pigments, 136*, 887-892.

Oms-Oliu, G., Aguiló-Aguayo, I., Martín-Belloso, O., & Soliva-Fortuny, R. (2010). Effects of pulsed light treatments on quality and antioxidant properties of fresh-cut mushrooms. *Postharvest Biology and Technology, 56*, 216-222.

Pellicer, J. A., & Gómez-López, V.M. (2017). Pulsed light inactivation of horseradish peroxidase and associated structural changes. *Food Chemistry, 237*, 632-637.

Siddique, M.A.B., Maresca, P., Pataro, G., & Ferrari, G. (2017). Influence of pulsed light treatment on the aggregation of whey protein isolate. *Food Research International, 99*, 419-425.

Turoverov, K.K., Hitlina, S.Y., & Pinaev, G.P. (1976). Ultra-violet fluorescence of actin. Determination of native actin content in actin preparations. *FEBS Letters, 62*(1), 4-6.

Vivian, J.T., & Callis, P.R. (2001). Mechanism of tryptophan fluorescence shifts in proteins. *Biophysical Journal, 80,* 2093-2109.

FIGURE LEGENDS

Fig. 1. Schematic representation of the PL system used to inactivate PPO.

Fig. 2. Inactivation of PPO by PL. Results are the mean of three independent experiments. Bars represent standard deviations, which are sometimes too small to be observed.

Fig. 3. Steady-state tryptophan fluorescence evolution during PPO inactivation by PL.

Fig. 4. Parameter A evolution during PPO inactivation by PL. Bars represent standard deviations.

Fig. 5. Correlation between PPO inactivation and parameter A. Bars represent standard deviations.

Fig. 6. Phase diagram analysis of PL-induced changes of PPO based on intrinsic fluorescence intensity values measured on wavelengths 320 and 365 nm.

Table 1. Stern-Volmer constants for fluorescence quenching by KI and turbidity index after PL treatment of PPO.

Fluence (J/cm^2)	K_{SV} (M^{-1})	Turbidity index
0	0.39 ± 0.16^a	0.039±0.010*
21	----	0.042±0.012
43	----	0.039±0.014
64	0.38 ± 0.17^a	0.040±0.012
86	----	0.040±0.016
107	----	0.041±0.011
128	0.76 ± 0.14^b	0.039±0.013

[ab] K_{SV} values with different superscripts are statistically different ($P<0.05$).
* Turbidity values are not statistically significant ($P>0.05$).

Figure 1

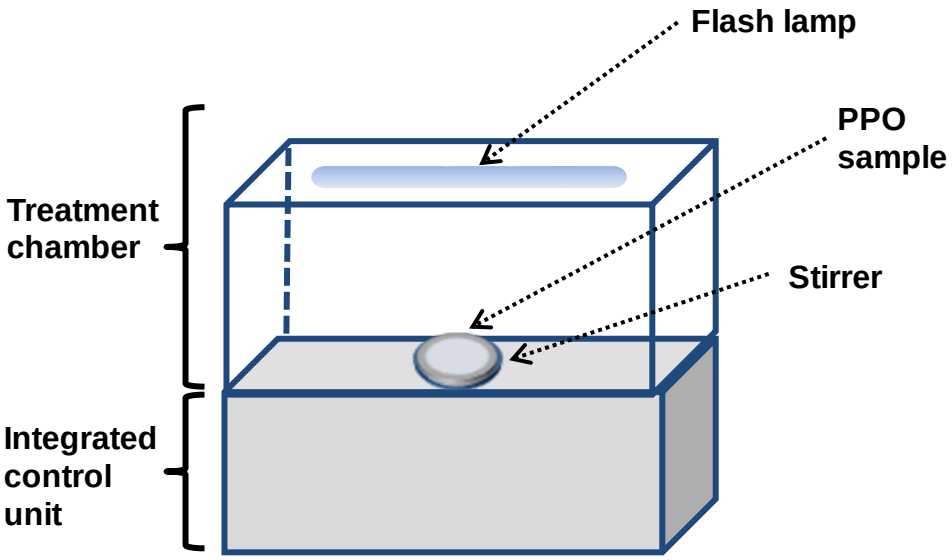
Flash lamp
PPO sample
Stirrer
Treatment chamber
Integrated control unit

Figure 2

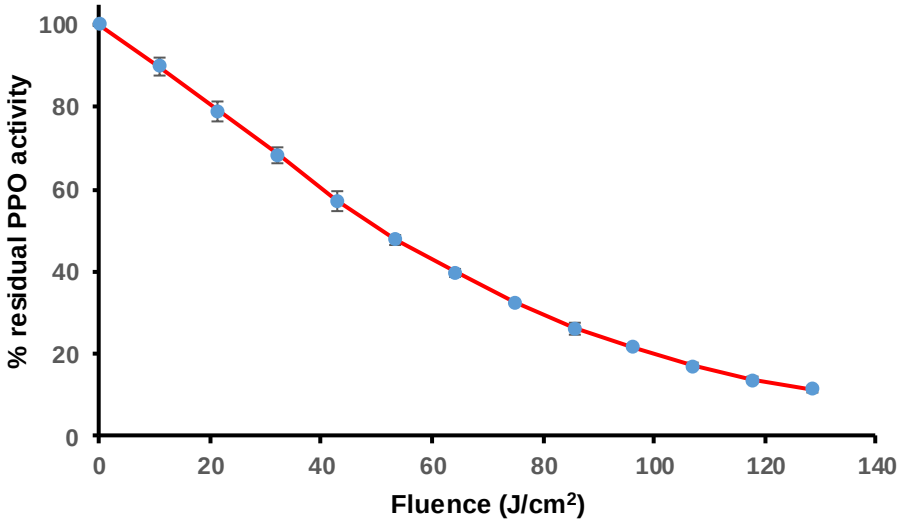
% residual PPO activity
100
80
60
40
20
0
0
20
40
60
80
100
120
140
Fluence (J/cm²)

Figure 3

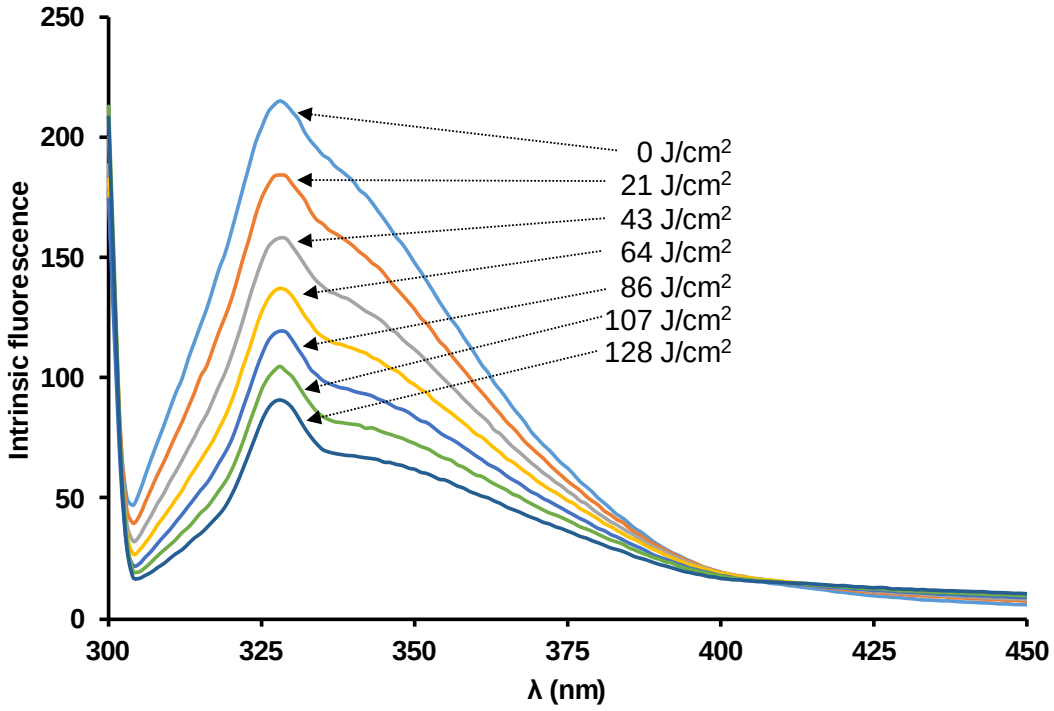
250
200
150
100
50
0
Intrinsic fluorescence
300
325
350
375
400
425
450
λ (nm)
0 J/cm2
21 J/cm2
43 J/cm2
64 J/cm2
86 J/cm2
107 J/cm2
128 J/cm2

Figure 4

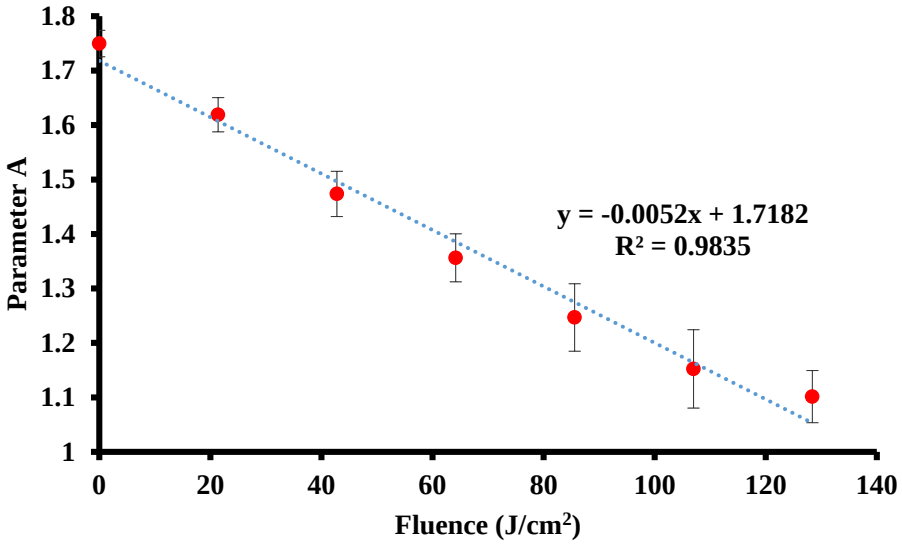
1.8
1.7
1.6
1.5
1.4
1.3
1.2
1.1
1
Parameter A
0
20
40
60
80
100
120
140
Fluence (J/cm²)
y = -0.0052x + 1.7182
R² = 0.9835

Figure 5

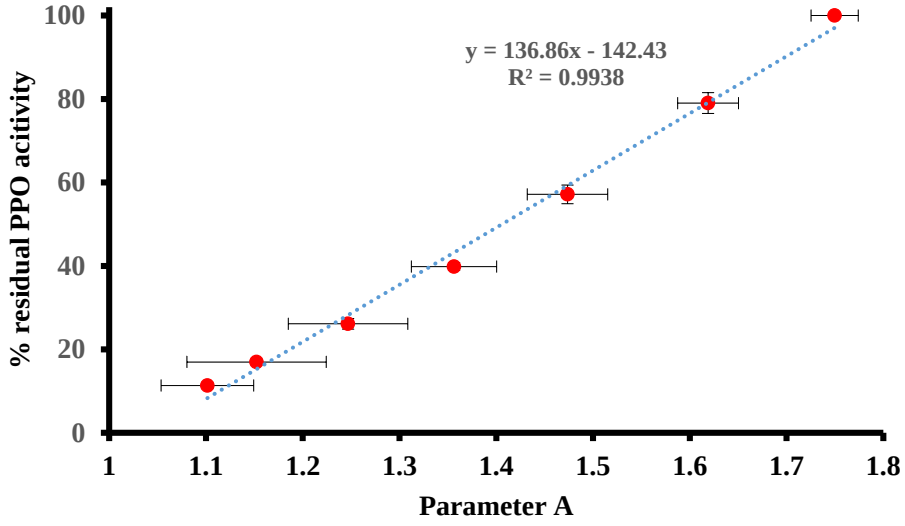
y = 136.86x - 142.43
R² = 0.9938
% residual PPO acitivity
Parameter A
0
20
40
60
80
100
1
1.1
1.2
1.3
1.4
1.5
1.6
1.7
1.8

Figure 6

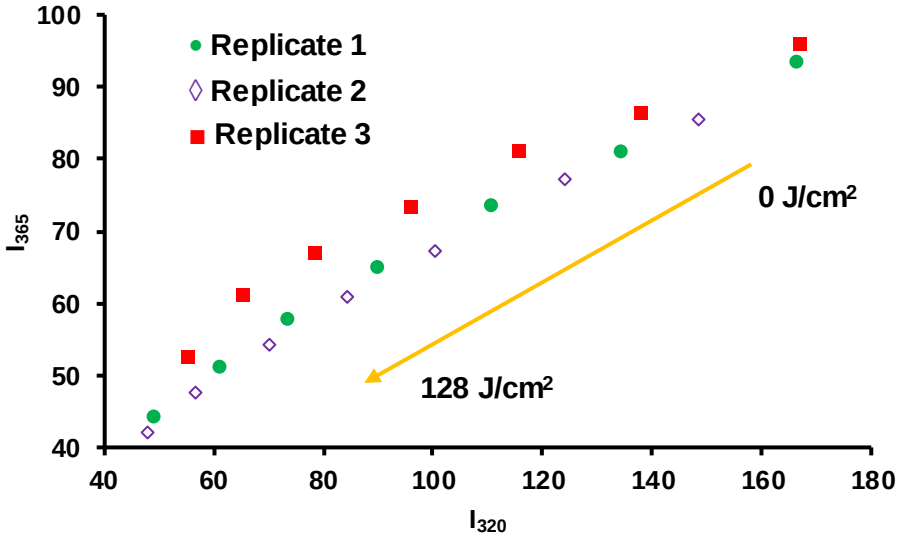
Replicate 1
Replicate 2
Replicate 3
0 J/cm²
128 J/cm²
I365
I320
100
90
80
70
60
50
40
40
60
80
100
120
140
160
180